Cobalt-Catalyzed Enantioselective C-H Arylation of Indoles

Nicolas Jacob, Yassir Zaid, João C A Oliveira, Lutz Ackermann, Joanna Wencel-Delord

Cobalt-Catalyzed Enantioselective C-H Arylation of Indoles

Nicolas Jacob,[1] Yassir Zaid,[1] João C.A. Oliveira,[2] Lutz Ackermann,[2,3]* and Joanna Wencel-Delord[1]*

[1]Laboratoire d'Innovation Moléculaire et Applications (UMR CNRS 7042), Université de Strasbourg/Université de Haute-Alsace, ECPM, 67087 Strasbourg, France

[2]Institut für Organische und Biomolekulare Chemie, Georg-August-Universität Göttingen, Tammanstraße 2, 37077 Göttingen, Germany

[3]Wöhler Research Institute for Sustainable Chemistry (WISCh), Georg-August-Universität Göttingen, Tammanstraße 2, 37077 Göttingen, Germany

KEYWORDS: C-H activation, axial chirality, arylation, cobalt, heterobiaryls, catalysis, atropoisomerism, indole, DFT calculations, mechanism.

ABSTRACT: Atropoisomeric (hetero)biaryls are scaffolds with increasing importance in the pharmaceutical and agrochemical industries. Although it is the most obvious disconnection to construct such compounds, the direct enantioselective C-H arylation through the concomitant induction of the chiral information remains extremely challenging and uncommon. Herein, the unprecedented earth-abundant 3d-metal-catalyzed atroposelective direct arylation is reported, furnishing rare atropoisomeric C2-arylated indoles. Kinetic studies and DFT computation revealed an uncommon mechanism for this asymmetric transformation, with the oxidative addition being the rate- and enantio-determining step. Excellent stereoselectivities were reached (up to 96% *ee*), while using an unusual *N*-heterocyclic carbene-ligand bearing essential remote substituent. Attractive dispersion interactions along with positive C-H---π interactions exerted by the ligand were identified as key factors to guarantee the excellent enantioselection.

INTRODUCTION

Medicinal chemistry and drug design are in a constant quest for new three-dimensional motifs, providing appealing biological activities and specific interactions with the targeted biological sites.[1] For decades, the introduction of stereogenic carbons was used to implement three-dimensionality within the drug candidates, thus giving the promise of advanced and more selective interactions with enzymatic sites.[2] During the recent years, significant attention has shifted to the implementation of atropoisomers within the drug design (**Figure 1A**).[3] Indeed, the presence of biaryl units featuring restricted rotation around an Ar-Ar axis and thus, exhibiting stable three-dimensional structure, frequently accounts for significantly improved biological activities and fewer side effects. In addition, applications of atropoisomerism to crop protection and material sciences, in combination with asymmetric catalysis further highlight the fascinating features of this chiral motif.

With the rapidly increasing importance of atropoisomerism in both fundamental research and industrial settings, the design of new atropoisomeric scaffolds together with efficient, rapid and sustainable strategies are in urgent need. While various approaches have recently burgeoned to complement the classical protocols for asymmetric atroposelective synthesis,[4] including Suzuki-Miyaura couplings and oxidative arylations, C-H activation-based strategies[5] are particularly attractive in terms of sustainability, access to simple starting materials, and generality. In this context, atroposelective *ortho*-C-H functionalization of pre-existing biaryl substrates have established themselves as an attractive route to diversified chiral biaryls and heterobiaryls (**Figure 1B**).[6,7] Examples of C-H couplings with highly reactive diazo-compounds have also been reported.[8] In sharp contrast, synthetic routes based on direct atroposelective Ar-H/Ar-X coupling remain hardly explored.[9] The challenging character of this transformation arises from the antagonism between, on the one hand, the essential steric hindrance of both coupling partners required to warrant the atropostability of the newly generated Ar-Ar products, and, on the other hand, exceedingly mild reaction conditions necessary to enable high stereoinduction and avoid *in-situ* racemization. While a pioneering contribution has

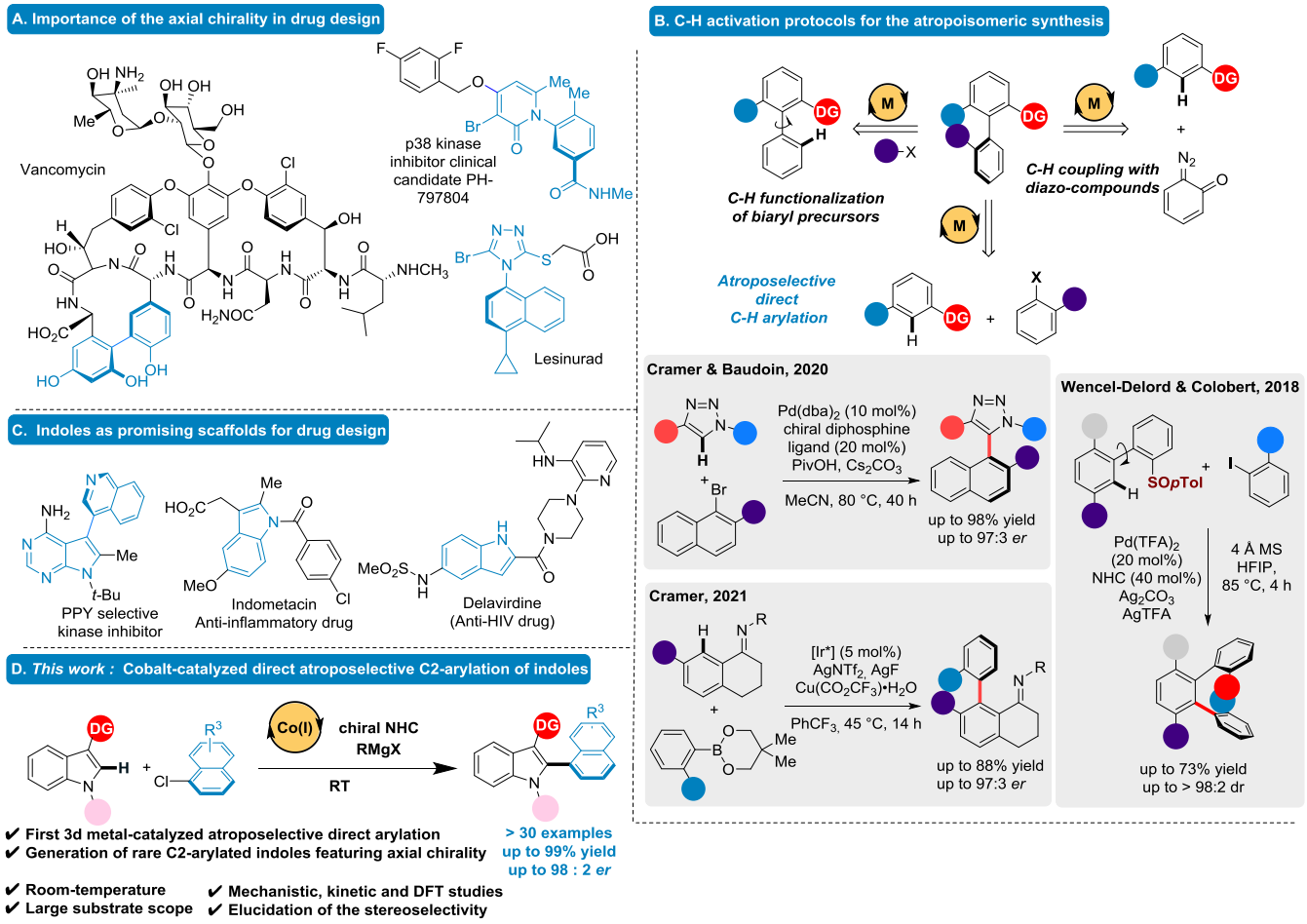

Figure 1. Towards new sustainable assembly of atropoisomeric C2-arylated indoles

been reported by the groups of Yamaguchi and Itami,[10] the application of the catalytic system remained rather limited. Wencel-Delord and Colobert reported atropodiastereoselective arylation delivering terphenyl compounds with two fully controlled chiral axes,[11] while the first truly efficient enantioselective system was very recently reported by Baudoin and Cramer.[12] Further, the portfolio of atroposelective C-H couplings has been complemented with iridium-catalyzed arylation of naphthylimines.[13] However, all these catalytic systems are severely limited by the use of precious palladium or iridium catalysts, while sustainable approaches benefiting from the exploitation of inexpensive and less toxic earth-abundant 3d-metals remain unprecedented.[14]

The use of 3d-transition metals in the C-H activation arena has strongly induced the recent development of this field as not only being more sustainable, less expensive, and environmentally benign catalysts, but also new mechanistic scenarios are frequently viable.[15] In particular, unprecedented reactivity may be reached with cobalt-based catalysts.[16] Hence, while high-valent cobalt(III) species tend to often perform rather similarly to rhodium(III) complexes, the mechanistic scenario based on low-valent cobalt intermediates is largely underexplored.[17] Due to the increased reactivity of the low-valent cobalt species towards the key C-H metalation step,[18] cobalt(I)-catalyzed transformations generally occur at lower, close to room temperatures, thus offering unique perspectives for atroposelective functionalizations. However, despite recent advances in implementing 3d-metal catalysis within stereo-controlled direct functionalizations,[14] only a single example of the enantioselective low-valent cobalt-catalyzed C-H activation has been reported, delivering C-stereogenic indole derivatives with moderate to good *ees* (up to 93.5:6.5 *er*).[19,20] Besides, a handle of enantioselective cobalt(III)-catalyzed reactions further illustrates the importance and challenging character of this field.[21]

Based on this analysis, we hypothesized that directed, cobalt(I)-catalyzed atroposelective C2-arylation of indoles should be feasible under mild reaction conditions, thereby delivering biaryls bearing a five-membered cycle.[4b] The development of such an unprecedented cobalt-catalyzed direct indole arylation also delineates a great prospect from a medicinal chemistry viewpoint. Indeed, indoles are amongst the key motifs in medicinal chemistry, frequently found in antiviral agents, kinase inhibitors or anticancer agents, among others (**Figure 1C**).[22] However, although strategies are available to construct atroposelectively C3-arylindoles,[23] the enantioselective synthesis of their C2-functionalized congeners remains underdeveloped. Rare and very recently disclosed approaches consist in central-to-axial chirality transfer[24] or stereoselective formation of the aromatic ring,[25] thus requiring finely designed substrates and catalysts. The development of significantly

more user-friendly strategies benefiting from non-functionalized indole substrates, together with inexpensive and abundant catalysts, is thus urgently needed to provide innovative structures for biological studies.

RESULTS AND DISUSSIONS

Reaction development At the outset (**Figure 1D**), we hypothesized that indole **1a** might be a suitable substrate for atroposelective cobalt-catalyzed direct C2-arylation. Indeed, the presence of the methyl group on the *N*-atom should limit its coordinating properties and bring about the steric hindrance necessary for the room-temperature atropostability of the newly generated Ar-Ar linkage. The imine substituent at the C3 position should enable chelation assistance, facilitating regioselective C2-metallation.[26] 1-chloronaphthalene **2a** was selected as the substrate to ensure atropostability of the newly generated product, while catalytically active cobalt(I) was *in-situ* generated *via* reduction of $CoBr_2$. Orienting experiments showed chiral *N*-heterocyclic carbene precursors (NHC)[27] as uniquely effective chiral inductors (**Figure 2**). Despite initial disappointing enantio-inductions observed with standard NHCs, such as **L1**, **L2** and **L3**, a remarkable improvement was achieved in the presence of **L4**, previously optimized for asymmetric iron-catalyzed C-H activation.[28]

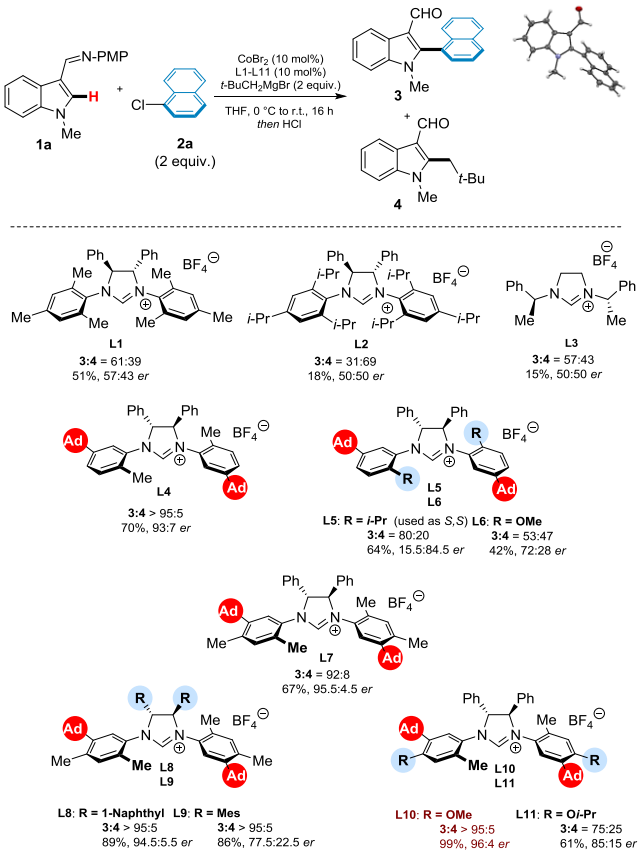

Figure 2. Ligand optimization. Reaction conditions: indole (1 equiv.), 1-chloronaphthalene (2 equiv.), $CoBr_2$ (10 mol%), ligand (10 mol%), *t*-$BuCH_2MgBr$ (2 equiv.) and THF (0.28 M), 0 °C to r.t., 16 h. Ratio between **3** and **4** was determined by ^1H NMR analysis of the crude reaction mixture. The yields refer to isolated product and the *ee* values were determined by HPLC with a chiral column.

A combination of this *meta*-adamantyl substituted ligand and $CoBr_2$ furnished the desired product **3** in an exceptional 93:7 *er* and 70% isolated yield, with only a trace amount of the undesired side product **4** being generated. Based on this outstanding starting point, the structure of the ligand **L4** was further probed. While replacing the *ortho*-substituent by more hindered *iso*-propyl or less sterically encumbered methoxy motifs (**L5** and **L6**, respectively), a significant drop in chiral induction was observed. In contrast, an excellent enantioselectivity of 95.5:4.5 *er* was reached while introducing an additional methyl-substituent in the *para*-position of the aromatic ring (**L7**). Modification of the chiral backbone did not improve further the chiral induction; a comparable enantioselectivity was observed with NHC **L8** bearing 1-naphthyl substituent, but mesityl-substituted **L9** was clearly less selective. Finally, the optimal chiral induction of 92% *ee* and 99% isolated yield were obtained while further increasing the electron-donating properties of the ligand by introducing a methoxy-group in the *para*-position (**L10**). Of note is that other reaction parameters, such as the cobalt precursor or the nature of a coordinating solvent poorly impacted the reaction outcome, while the selection of the reducing base was crucial for the efficiency of the catalytic system (see SI).

Scope With the optimized reaction conditions in hand, the generality of this atroposelective direct arylation was challenged (**Figure 3**). First, differently *N*-substituted indoles (**1a-v**) were reacted with 1-chloronaphthalene **2a** under otherwise identical reaction conditions. Dioxolane and benzyl-protected indoles underwent the desired transformation, affording products **6** and **7** with high enantioselectivities. In contrast, the presence of a MOM group seemed inadequate. PMB-substituted indole performed equally well and furnished indole **9** with 96:4 *er*, while slightly lower chiral induction (93.5:6.5 *er*) was observed for the product **8** bearing a phenyl-substituent.

Subsequently, the reaction was performed in the presence of different 1-chloronaphthalenes (**10**-**18**), bearing various functionalities. Electron-donating groups at the 4-position of the 1-chloronaphthalene only slightly impacted the atroposelectivity of the reaction (products **10**, **11** and **12**). The optimal enantiomeric ratio was obtained when using the fluorinated substrate, delivering **15** with 98:2 *er* and 54% yield. Interestingly, an extension of the polyaromatic system to 1-chlorophenanthrene provided **16** in high yield and 90:10 *er* but a significant drop of chiral induction occurred when using 1-chloropyrene **2i**. Moreover, due to the too high steric hindrance, the C-H coupling was not effective when 2-substituted 1-chloronaphthalene **2j** was used, even upon heating at 60 °C (product **18**). Finally, *o*-chlorotoluene **2k** is also a potent substrate, but product **19** was isolated in 61% yield and a lower enantioselectivity (77:23 *er*).

Remarkably, the catalytic system showed high compatibility with an array of functionalized indoles (**1f-v**). Both electron-rich and electron-poor substituents could thus be installed at different positions of the carbocycle, while only modestly impacting atroposelective outcome of the transformation. Importantly, thioether- and thiophene-substituted products **26** and **27** could be isolated in 88%

and 82% yields, and 95.5:4.5 and 93.5:6.5 *er*, respectively. Notably, the compatibility with different fluorinated groups, including F, CF_3, OCF_3 and SF_5 (products **22**, **29-32**, **34**) should represent key advantage from a medicinal chemistry viewpoint. Worth highlighting is also the efficiency of this C-H arylation with the azaindole substrate, affording the chiral product **35** with excellent yield and *er*.

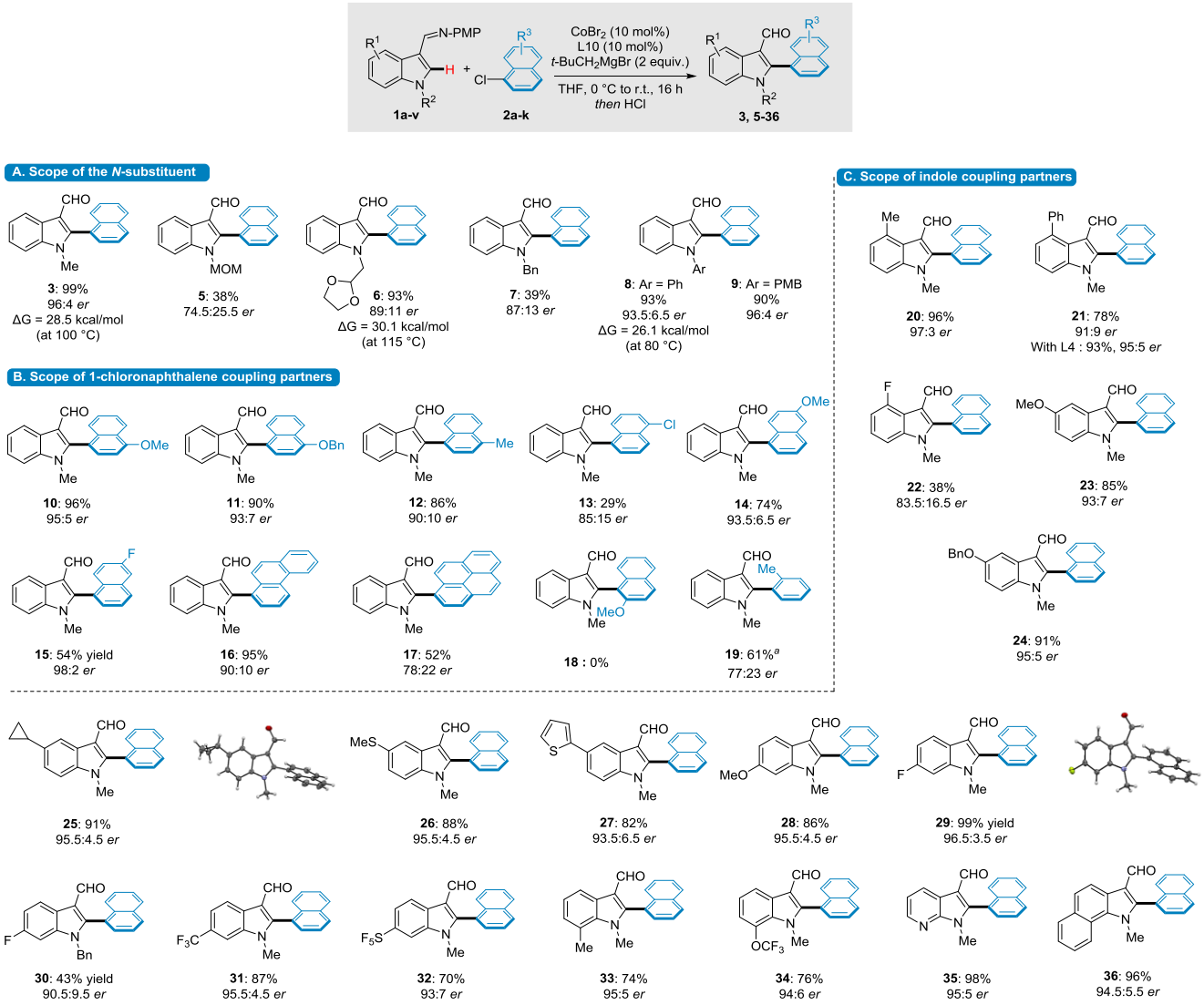

Figure 3. Scope of the atropoenantioselective indoles arylation. For general reaction conditions, see Figure 2. [a]60 h reaction time.

To characterize the newly synthesized compounds, the rotational barriers were experimentally determined. Product **3** features a rotational barrier of 28.5 kcal mol^{-1} at 100 °C, as was experimentally determined (estimated by DFT calculations: 29.8 kcal mol^{-1}, **Table S9**) thus no racemization occurs at room temperature on a month's scale. A higher rotational barrier of 30.0 kcal mol^{-1} was observed for indole **6**, indicating increased steric hindrance induced by the dioxolane motif. In clear contrast, the presence of phenyl-group on the *N*-atom translates into significantly atropostability decrease of **8** to only 26.0 kcal mol^{-1} (at 80 °C); generation of this compound in atropoisomerically pure form would not be possible under higher reaction temperatures, since at 110 °C, the racemization occurs within only 5 min.

To further explore the synthetic potential of our strategy, a large-scale reaction was performed, furnishing the expected product **3** in unchanged optical purity (**Figure 4A**). Interestingly, hydrolysis of the imine directing group is not necessary and atropoisomerically pure imine-indole **37** could be isolated in an optical purity of 95:5 *er* and excellent yield. Importantly, simple recrystallization further increased the optical purity of the compound **3** to afford efficiently 99:1 *er* with 62% yield. Finally, to explore the synthetic potential of our new chiral building blocks, different post-modifications have been performed using compound **3** as a substrate. First, different transformations of the formyl moiety have been carried out. Reduction of aldehyde **3** occurred efficiently, furnishing the corresponding alcohol **38**. Reductive amination using methylamine performed well, affording product **39**. Notably, a Wittig reaction led to product **40**. Aldehyde **3** reacted also with different Grignard reagents, thereby delivering the corresponding alcohols **41** and **42** with low to moderate diastereoselectivities and excellent yields. Both diastereoisomers could be separated by simple column

chromatography. It is worth noting that all these transformations occurred without erosion of the optical purity of the chiral C-C axis. Finally, we took advantage of the presence of the formyl group as a weakly coordinating group to enhance C4-direct functionalization *via* C4 rhodium(III)-catalyzed direct alkylation,[29] Product **43** could thus be synthesized in a good yield and without racemization of the atropisomeric axis. Subsequent intramolecular crotonization led to 3,4-fused tricyclic indole **44**. The product **44** features a decreased steric hindrance around the Ar-Ar bond, translating into the lost of the chiral information (racemization within less than 24 hours). Ultimately, a double-Wittig reaction efficiently furnished diene **45** in 96% *ee*. (**Figure 4B**).

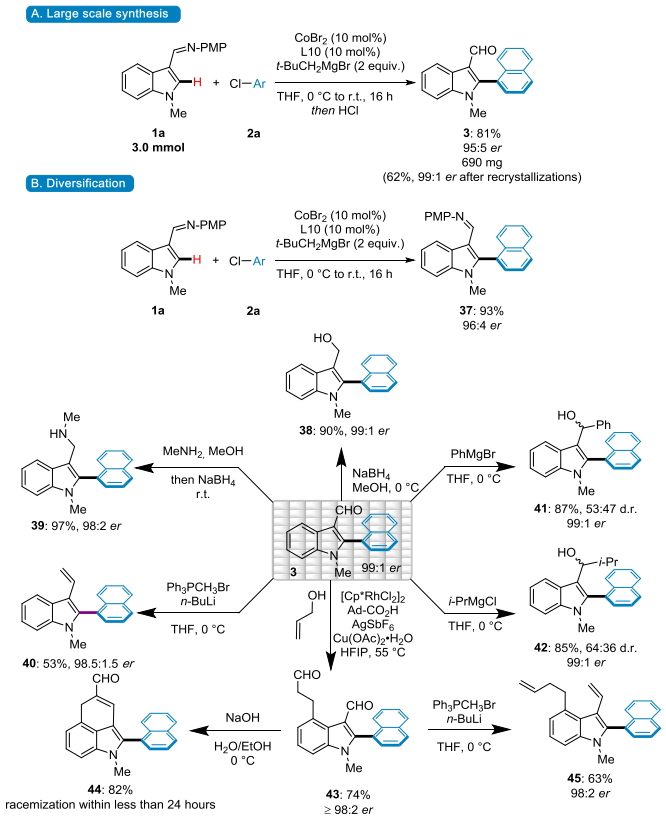

Figure 4. Diversification of the generated atropoisomeric compounds.

Mechanistic Studies Considering the relatively limited mechanistic understanding of the low-valent cobalt-catalyzed C-H arylation, we endeavored on detailed mechanistic and kinetic investigations combining experimental investigations with DFT calculations.

First, detailed kinetic studies have been performed (**Figure 5**). The kinetic isotope effect (KIE) study (competitive experiment and initial rate determination) indicated a KIE value close to 1, thus clearly suggesting that the C-H activation step is not the rate-determining step (**Figure 5A**). This finding corroborates previous investigations on the cobalt(I)-catalyzed C-H activation.[18] Then, qualitative *in operando* infrared spectroscopy unrevealed an extremely fast character of the direct arylation during the first half-hour of the reaction (**Figure 5B**). Indeed, the C-H activation reaction furnished product **3** in 65% isolated yield after only 30 min at 0 °C. However, an increased reaction time is necessary to reach full conversion of the starting material. Analysis of the initial reaction rate (**Figure 5C**) revealed a zeroth order in the concentration of indole. In contrast, the reaction rate was depending on the concentration of 1-chloronaphthalene **2a** according to a first order dependence, with saturation kinetics.

Next, DFT calculations for the oxidative addition and reductive elimination elementary steps were carried out at the PW6B95-D4/def2-TZVP+SMD(THF)//TPSS-D3(BJ)/def2-SVP level of theory (**Figure 6** and **Figures S5-S9**, for detailed information see SI).[30] Given the d^8-electronic configuration of the cobalt(I) intermediates **I-1**, both high-spin (triplet) and low-spin (singlet) complexes were taken into consideration for both the (*R*)- and the (*S*)-enantiomers for the C–H activation and oxidative addition steps through transition states **TS(1-2)** and **TS(2-3)** respectively (**Figures S5** and **S6**).[31] This gives rise to cobalt(III) complexes **I-4**, which undergo reductive elimination through **TS(4-5)** (**Figures S5** and **S6**). For the cobalt(III) complexes the possible singlet, triplet, quintet spin states were assessed. The extensive analysis of the possible spin states highlighted the triplet surface as the energetically favored pathway for both enantiomers with no spin-crossover reactivity. A comparison between the most energetically favored triplet surfaces of (*R*)- and (*S*)-enantiomers is disclosed on **Figure 6.**

C–H activation was found to be facile with an activation energy of only 5 kcal mol^{-1} suggesting that the C–H activation step is not rate-determining. This is in good agreement with the experimental findings, highlighting the robustness and suitability of the computational method approach.

Calculations indicated that oxidative addition proceeds through a barrier of 9.3 kcal mol^{-1} for the experimentally observed (*S*)-enantiomer which is stabilized by 0.7 kcal mol^{-1} over the (*R*)-enantiomer.

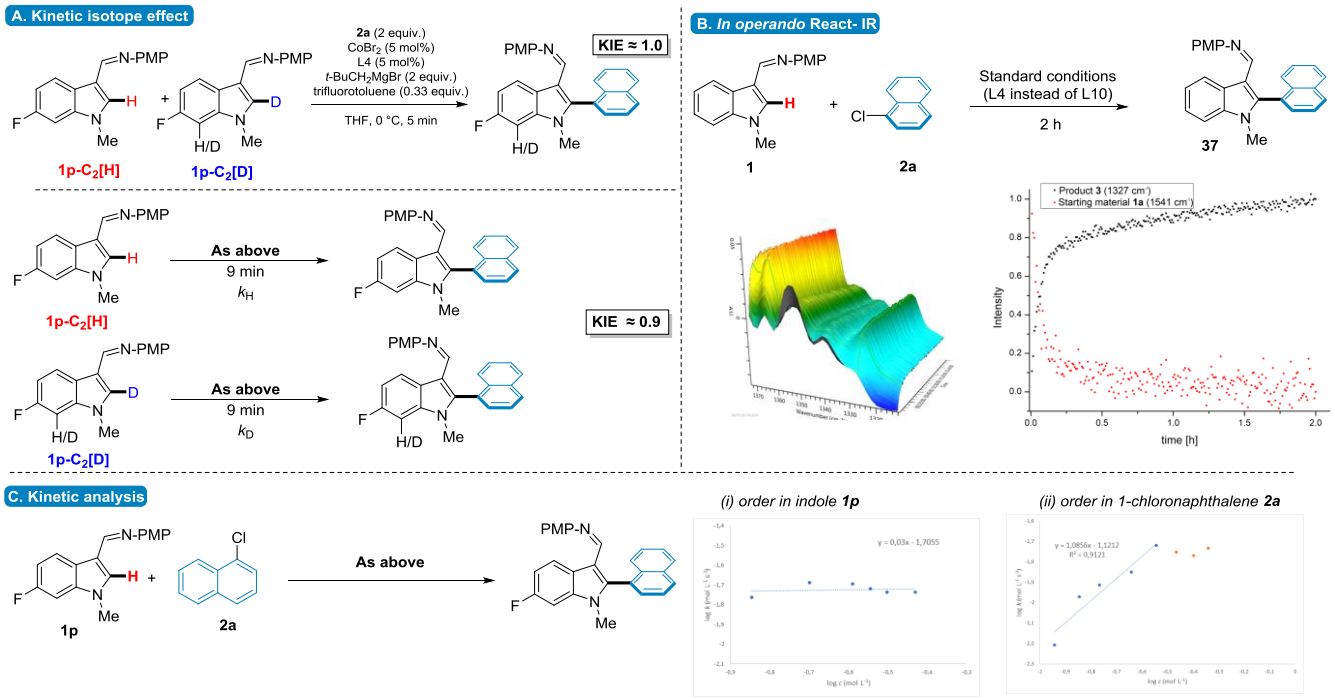

Figure 5. Kinetic studies

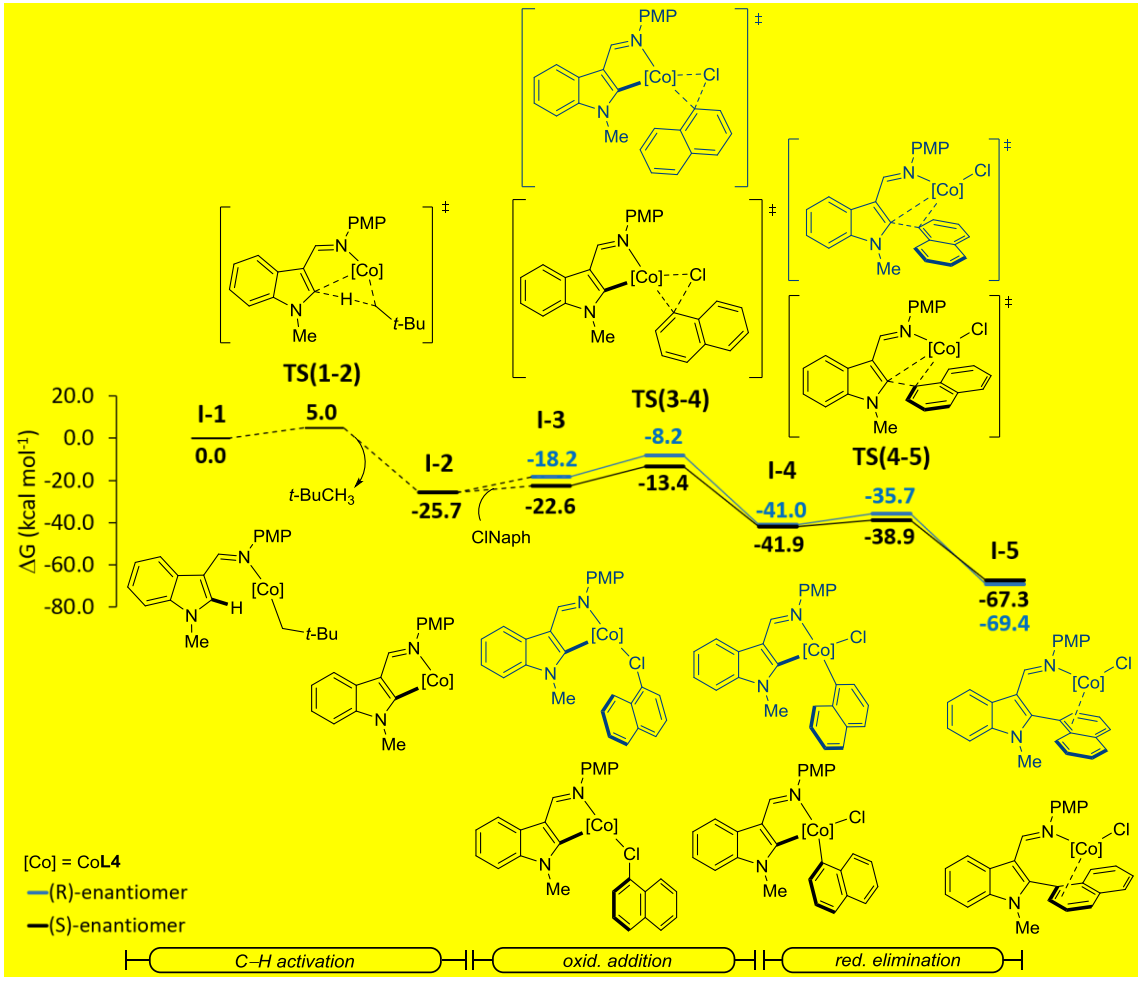

Figure 6. Computed relative Gibbs free energies ($\Delta G_{273.15}$) in kcal mol^{-1} between C–H activation and reductive elimination elementary steps, in the most stable triplet surface, for the (*R*)- and (*S*)-enantiomers at the PW6B95-D4/def2-TZVP+SMD(THF)//TPSS-D3(BJ)/def2-SVP level of theory with the chiral ligand **L4.**

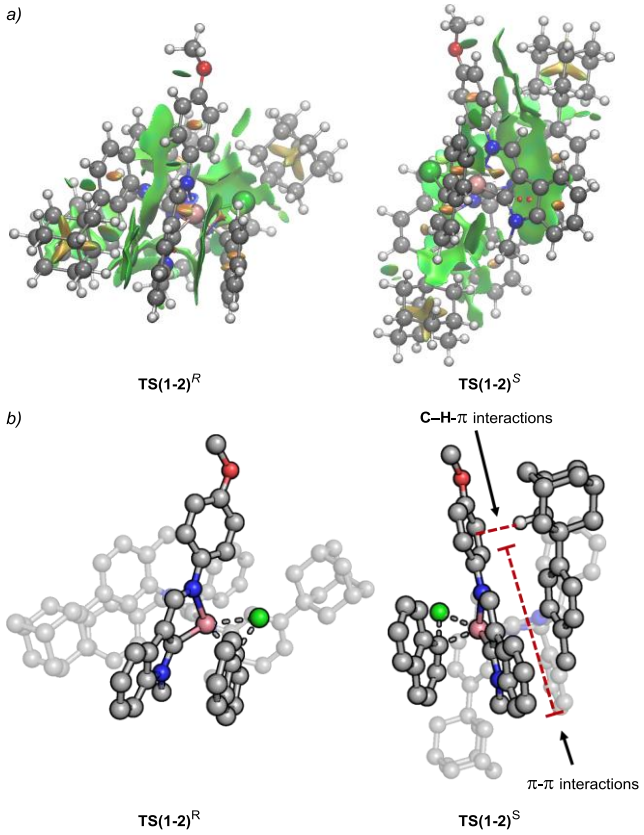

Figure 7. a) Visualisation of the non-covalent interactions calculated with the help of the NCIPLOT program for the transition states involved in the oxidative addition step for both (*R*)- and (*S*)-enantiomers. In the plotted surfaces, red corresponds to strong repulsive interactions, while green and blue correspond to weak and strong interactions, respectively. Superscripts *R* and *S* correspond to the (*R*)- and (*S*)-enantiomers respectively. b) Identification of relevant interactions in the transition state structures, for the oxidative addition elementary step in the triplet surface, for the (*R*)- and (*S*)-enantiomers obtained at the TPSS-D3(BJ)/def2-SVP level of theory with the chiral ligand **L4**. Non-relevant hydrogens were omitted for clarity. Superscripts *R* and *S* correspond to the (*R*)- and (*S*)-enantiomers respectively.

This stabilization is found to result from attractive dispersion interactions of the substrate and the *meta*-aryl substituent of the remote NHC ligand, which is more pronounced in the (*S*)-enantiomer transition state structure (**Figure 7a**). These are mostly localized in the region defined by the plane of the NHC substituted moiety and the substrate that is parallelly orientated (**Figure 7b**). Additionally, the presence of positive CH---π interactions between the adamantyl group from the NHC side-chain and the *para*-methoxyphenyl moiety of the substrate contributes to the stabilization of the transition state structure **TS(3-4)^S** over the **TS(3-4)^R** (**Figure 7a-b**), highlighting the intrinsic ability of the *meta*-adamantyl-substituted ligand **L4** to serve as a remote dispersion energy donor.[32] To support such observation, calculations were also performed in the absence of dispersion corrections at the PW6B95/def2-TZVP+SMD(THF)//TPSS/def2-TZVP level of theory. A direct comparison between the TPSS and TPSS-D3(BJ) data was carried out in terms of NBO and NCIPLOT analysis. The NCIPLOT analysis in the absence of dispersion corrections revealed a decrease in the weak attractive surface for both (*R*)- and (*S*)-enantiomers (**Figure S10**). The direct comparison between calculations in the absence and in the presence of dispersion corrections revealed in the second-order perturbation theory of the Fock matrix within the NBO analysis (**Table S13-S16**) for **TS(3-4)** of (*S*)-enantiomer a stabilization of 1.1 kcal mol^{-1} when dispersion effects were considered. In contrast, for the (*R*)-enantiomer, only a stabilization of 0.5 kcal mol^{-1} was observed. These results support that dispersion interactions play an important role in the stabilization of **TS(3-4)^S**.

During the reductive elimination (**TS(4-5)**) the (*S*)-enantiomer is 3.2 kcal mol^{-1} more stable than the (*R*)-enantiomer. Our results demonstrate the oxidative addition to be the rate-determining step and responsible for the enantioinduction. The energy gap of 0.7 kcal mol^{-1} in **TS(3-4)** between the two enantiomers results in an *ee* of 72% in favor of the (*S*)-enantiomer, as was observed experimentally. The minor difference to the experimentally found *ee* of 86%, i.e. 1.1 kcal mol^{-1}, can be rationalized by secondary solvent effects.

Based on detailed DFT analysis and in accordance with experimental mechanistic investigations, a plausible catalytic cycle as is proposed in **Figure 8**. First, the catalytically active cobalt(I) species is generated *via* reduction by the base and the coordination with the imine delivers intermediate **A**. The C-H metalation step is fast, affording the metallacycle **B**. Subsequent stereo- and rate-determining oxidative addition takes place delivering cobalt(III)-intermediate **C**, while the expected enantiopure product is released *via* reductive elimination, along with ligand exchange.

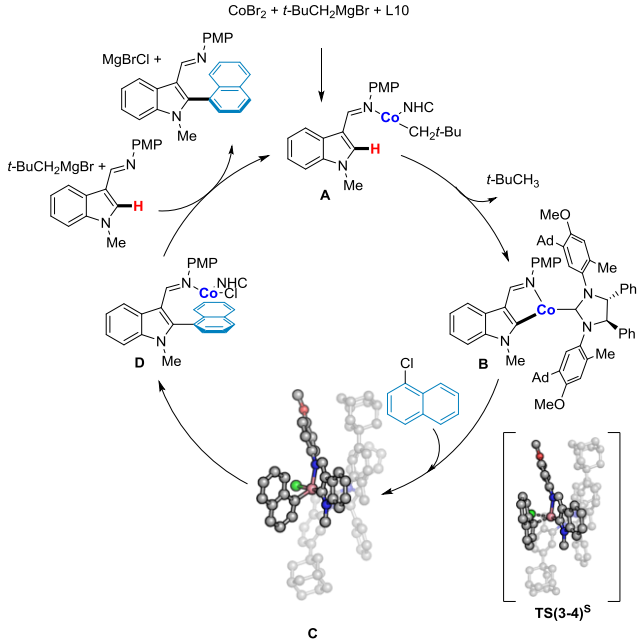

Figure 8. Proposed catalytic cycle

CONCLUSIONS

In conclusion, we have reported the first atropoenantioselective cobalt-catalyzed C-H arylation to deliver rare atropoenriched C2-arylated indoles. The high reactivity of the cobalt(I) species enables an efficient C-H arylation at room temperature, thus guaranteeing atropostability of the newly generated compounds. Carbene ligands presenting remote *meta*-dispersion donor motifs were found to be essential for the stereoselectivity, as rationalized by detailed DFT calculations, elucidating for the first time a stereoselection rationale for the atroposelective 3d-metal catalyzed C-H arylation.

ASSOCIATED CONTENT

Supporting Information.
The supporting information is available free of charge on the ACS Publications website.
Accession codes.
CCDC 2086165, 2086166 and 2086167 contain the supplementary crystallographic data for this paper. These data can be obtained free of charge *via* www.ccdc.cam.ac.uk/data_request/cif, or by emailing data_request@ccdc.cam.ac.uk, or by contacting The Cambridge Crystallographic Data Centre, 12 Union Road, Cambridge CB2 1EZ, UK; fax: +44 1223 336033.

AUTHOR INFORMATION

Corresponding Authors

Lutz.Ackermann@chemie.uni-goettingen.de
wenceldelord@unistra.fr

Author Contributions

The manuscript was written through contributions of all authors.

ACKNOWLEDGMENT

J.W.-D. thanks the CNRS (Centre National de la Recherche Scientifique), the « Ministère de l'Éducation Nationale et de la Recherche » (France) for financial support. J.W.-D., L.A. and N. J. acknowledge ANR (Agence Nationale de la Recherche) and DFG collaborative project ANR PRCI (grant number ANR-17-CE07-0049-01). L.A. thanks the DFG (SPP 1807, AC 118/9-1). Y.Z. is very grateful to ANR for the postdoctoral fellowship (project ANR-ERC-T « Alchimie »). We are also very grateful to Dr. Lydia Karmazin, Dr. Corinne Bailly and Nathalie Gruber for single crystal X-ray diffraction analysis.

REFERENCES

(1) (a) Battiti, F. O.; Cemaj, S. L.; Guerrero, A. M.; Shaik, A. B.; Lam, J.; Rais, R.; Slusher, B. S.; Deschamps, J. R.; Imler, G. H.; Newman, A. H.; Bonifazi, A. The Significance of Chirality in Drug Design and Synthesis of Bitopic Ligands as D_3 Receptor (D_3R) Selective Agonists. *J. Med. Chem.* **2019**, *62* (13), 6287–6314. (b) H. Brooks, W.; C. Guida, W.; G. Daniel, K. The Significance of Chirality in Drug Design and Development. *Curr. Top. Med. Chem.* **2011**, *11* (7), 760–770.
(2) (a) Sekhon, B. S. Exploiting the Power of Stereochemistry in Drugs: An Overview of Racemic and Enantiopure Drugs. *J. Mod. Med. Chem.* **2013**, *1*, 10-36. (b) Lovering, F.; Bikker, J.; Humblet, C. Escape from Flatland: Increasing Saturation as an Approach to Improving Clinical Success. *J. Med. Chem.* **2009**, *52* (21), 6752-6756.
(3) (a) Smyth, J. E.; Butler, N. M.; Keller, P. A. A twist of nature – the significance of atropisomers in biological systems. *Nat. Prod. Rep.* **2015**, *32* (11), 1562-1583. (b) Glunz, P. W. Recent encounters with atropisomerism in drug discovery. *Bioorg. Med. Chem. Lett.* **2018**, *28* (2) 53-60. (c) Toenjes, S. T.; Basilaia, M.; Gustafson, J L. Leveraging conformational control about a potential atropisomeric axis as a strategy in medicinal chemistry. *Future Med. Chem.* **2021**, *13* (5), 443-446.
(4) (a) Wencel-Delord, J.; Panossian, A.; Leroux, F. R.; Colobert, F. Recent advances and new concepts for the synthesis of axially stereoenriched biaryls. *Chem. Soc. Rev.* **2015**, *44* (11), 3418-3430. (b) Bonne, D.; Rodriguez, J. A Bird's Eye View of Atropisomers Featuring a Five-Membered Ring. *Eur. J. Org. Chem.* **2018**, 2417-2431. (c) Cheng, J. K.; Xiang, S.-H.; Li, S.; Ye, L.; Tan, B. Recent Advances in Catalytic Asymmetric Construction of Atropisomers. *Chem. Rev.* **2021**, *121* (8), 4805-4902. (d) Zilate, B.; Castrogiovanni, A.; Sparr, C. Catalyst-Controlled Stereoselective Synthesis of Atropisomers. *ACS Catal.* **2018**, *8* (4), 2981-2988.
(5) (a) Sambiagio, C.; Schönbauer, D.; Blieck, R.; Dao-Huy, T.; Pototschnig, G.; Schaaf, P.; Wiesinger, T.; Zia, M. F.; Wencel-Delord, J.; Besset, T.; Maes, B. U. W.; Schnürch, M. A Comprehensive Overview of Directing Groups Applied in Metal-Catalysed C–H Functionalisation Chemistry. *Chem. Soc. Rev.* **2018**, *47* (17), 6603–6743. (b) Dalton, T.; Faber, T.; Glorius, F. C–H Activation: Toward Sustainability and Applications. *ACS Cent. Sci.* **2021**, *7* (2), 245–261. (c) Lam, N. Y. S.; Wu, K.; Yu, J. Advancing the Logic of Chemical Synthesis: C-H Activation as Strategic and Tactical Disconnections for C-C Bon Construction. *Angew. Chem. Int. Ed.* **2021**, *60* (29), 15767-15790. (d) Rogge, T.; Kaplaneris, N.; Chatani, N.; Kim, J.; Chang, S.; Punji, B.; Schafer, L. L.; Musaev, D. G.; Wencel-Delord, J.; Roberts, C. A.; Sarpong, R.; Wilson, Z. E.; Brimble, M. A.; Johansson, M. J.; Ackermann, L. C–H Activation. *Nat Rev Methods Primers* **2021**, *1* (1), 43. (e) Liu, C.-X.; Zhang, W.-W.; Yin, S.-Y.; Gu, Q.; You, S.-L. Synthesis of Atropisomers by Transition-Metal-Catalyzed Asymmetric C–H Functionalization Reactions. *J. Am. Chem. Soc.* **2021**, *143* (35), 14025–14040.
(6) For a recent review see: Liao, G.; Zhou, T.; Yao, Q.-J.; Shi, B.-F. Recent Advances in the Synthesis of Axially Chiral Biaryls via Transition Metal-Catalysed Asymmetric C–H Functionalization. *Chem. Commun.* **2019**, *55* (59), 8514–8523.
(7) For the selected examples see: (a) Kakiuchi, F.; Le Gendre, P.; Yamada, A.; Ohtaki, H.; Murai, S. Atropselective Alkylation of Biaryl Compounds by Means of Transition Metal-Catalyzed C–H/Olefin Coupling. *Tetrahedron Asymmetry* **2000**, *11* (13), 2647–2651. (b) Yao, Q.-J.; Zhang, S.; Zhan, B.-B.; Shi, B.-F. Atroposelective Synthesis of Axially Chiral Biaryls by Palladium-Catalyzed Asymmetric C–H Olefination Enabled by a Transient Chiral Auxiliary. *Angew. Chem. Int. Ed.* **2017**, *56* (23), 6617–6621. (c) Zheng, J.; You, S.-L. Construction of Axial Chirality by Rhodium-Catalyzed Asymmetric Dehydrogenative Heck Coupling of Biaryl Compounds with Alkenes. *Angew. Chem. Int. Ed.* **2014**, *53* (48), 13244–13247. (d) Dhawa, U.; Tian, C.; Wdowik, T.; Oliveira, J. C. A.; Hao, J.; Ackermann, L. Enantioselective Pallada-Electrocatalyzed C–H Activation by Transient Directing Groups: Expedient Access to Helicenes. *Angew. Chem. Int. Ed.* **2020**, *59* (32), 13451–13457. (e) Hazra, C. K.; Dherbassy, Q.; Wencel-Delord, J.; Colobert, F. Synthesis of Axially Chiral Biaryls through Sulfoxide-Directed Asymmetric Mild C-H Activation and Dynamic Kinetic Resolution. *Angew. Chem. Int. Ed.* **2014**, *53* (50), 13871–13875.
(8) (a) Jia, Z.-J.; Merten, C.; Gontla, R.; Daniliuc, C. G.; Antonchick, A. P.; Waldmann, H. General Enantioselective C–H Activation with Efficiently Tunable Cyclopentadienyl Ligands. *Angew. Chem. Int. Ed.* **2017**, *56* (9), 2429–2434. (b) Kong, L.; Han, X.; Liu, S.; Zou, Y.; Lan, Y.; Li, X. Rhodium(III)-Catalyzed Asymmetric Access to Spirocycles through C–H Activation and Axial-to-Central Chirality Transfer. *Angew. Chem. Int. Ed.* **2020**, *59* (18), 7188–7192.
(9) Wencel-Delord, J.; Colobert, F. Challenging Atroposelective C–H Arylation. *SynOpen* **2020**, *04*, 107–115.
(10) Yamaguchi, K.; Yamaguchi, J.; Studer, A.; Itami, K. Hindered Biaryls by C–H Coupling: Bisoxazoline-Pd Catalysis Leading to Enantioselective C–H Coupling. *Chem. Sci.* **2012**, *3* (6), 2165–2169.
(11) Dherbassy, Q.; Djukic, J.-P.; Wencel-Delord, J.; Colobert, F. Two Stereoinduction Events in One C–H Activation Step: A Route towards Terphenyl Ligands with Two Atropisomeric Axes. *Angew. Chem. Int. Ed.* **2018**, *57* (17), 4668–4672.
(12) Nguyen, Q.-H.; Guo, S.-M.; Royal, T.; Baudoin, O.; Cramer, N. Intermolecular Palladium(0)-Catalyzed Atropo-Enantioselective C–H Arylation of Heteroarenes. *J. Am. Chem. Soc.* **2020**, *142* (5), 2161–2167.

(13) Woźniak, Ł.; Cramer, N. Atropo-Enantioselective Oxidation-Enabled Iridium(III)-Catalyzed C–H Arylations with Aryl Boronic Esters. *Angew. Chem. Int. Ed.* **2021**, *60* (34), 18532-18536.
(14) (a) Woźniak, Ł.; Cramer, N. Enantioselective C-H Bond Functionalizations by 3d Transition-Metal Catalysts. *Trends Chem.* **2019**, *1* (5), 471–484. (b) Loup, J.; Dhawa, U.; Pesciaioli, F.; Wencel-Delord, J.; Ackermann, L. Enantioselective C-H Activation with Earth-Abundant 3d Transition Metals. *Angew. Chem. Int. Ed.* **2019**, *58* (37), 2–18.
(15) Gandeepan, P.; Müller, T.; Zell, D.; Cera, G.; Warratz, S.; Ackermann, L. 3d Transition Metals for C–H Activation. *Chem. Rev.* **2018**, *119*, 2192–2452.
(16) (a) Moselage, M.; Li, J.; Ackermann, L. Cobalt-Catalyzed C–H Activation. *ACS Catal.* **2016**, *6* (2), 498–525. (b) Mei, R.; Dhawa, U.; Samanta, R. C.; Ma, W.; Wencel-Delord, J.; Ackermann, L. Cobalt-Catalyzed Oxidative C–H Activation: Strategies and Concepts. *ChemSusChem* **2020**, *13* (13), 3306-3356.
(17) (a) Gao, K.; Yoshikai, N. Low-Valent Cobalt Catalysis: New Opportunities for C–H Functionalization. *Acc. Chem. Res.* **2014**, *47* (4), 1208–1219. (b) Ackermann, L. Cobalt-Catalyzed C–H Arylations, Benzylations, and Alkylations with Organic Electrophiles and Beyond. *J. Org. Chem.* **2014**, *79* (19), 8948–8954.
(18) Oliveira, J. C. A.; Dhawa, U.; Ackermann, L. Insights into the Mechanism of Low-Valent Cobalt-Catalyzed C–H Activation. *ACS Catal.* **2021**, *11* (3), 1505–1515.
(19) Lee, P.-S.; Yoshikai, N. Cobalt-Catalyzed Enantioselective Directed C–H Alkylation of Indole with Styrenes. *Org. Lett.* **2015**, *17* (1), 22–25.
(20) For a rare example of cobalt(I)-catalyzed asymmetric hydroarylation, see: Whyte, A.; Torelli, A.; Mirabi, B.; Prieto, L.; Rodríguez, J. F.; Lautens, M. Cobalt-Catalyzed Enantioselective Hydroarylation of 1,6-Enynes. *J. Am. Chem. Soc.* **2020**, *142* (20), 9510–9517.
(21) (a) Ozols, K.; Onodera, S.; Woźniak, Ł.; Cramer, N. Cobalt(III)-Catalyzed Enantioselective Intermolecular Carboamination by C–H Functionalization. *Angew. Chem. Int. Ed.* **2021**, *60* (2), 655–659. (b) Kurihara, T.; Kojima, M.; Yoshino, T.; Matsunaga, S. Cp^*Co^{III}/Chiral Carboxylic Acid-Catalyzed Enantioselective 1,4-Addition Reactions of Indoles to Maleimides. *Asian J. Org. Chem.* **2020**, *9* (3), 368–371. (c) Liu, Y.-H.; Li, P.-X.; Yao, Q.-J.; Zhang, Z.-Z.; Huang, D.-Y.; Le, M. D.; Song, H.; Liu, L.; Shi, B.-F. Cp*Co(III)/MPAA-Catalyzed Enantioselective Amidation of Ferrocenes Directed by Thioamides under Mild Conditions. *Org. Lett.* **2019**, *21* (6), 1895–1899. (d) Pesciaioli, F.; Dhawa, U.; Oliveira, J. C. A.; Yin, R.; John, M.; Ackermann, L. Enantioselective Cobalt(III)-Catalyzed C–H Activation Enabled by Chiral Carboxylic Acid Cooperation. *Angew. Chem. Int. Ed.* **2018**, *57* (47), 15425–15429.
(22) (a) Zhang, M.-Z.; Chen, Q.; Yang, G.-F. A Review on Recent Developments of Indole-Containing Antiviral Agents. *Eur. J. Med. Chem.* **2015**, *89*, 421–441. (b) Sravanthi, T. V.; Manju, S. L. Indoles — A Promising Scaffold for Drug Development. *Eur. J. Pharm. Sci.* 2016, *91*, 1–10.
(23) (a) Li, T.-Z.; Liu, S.-J.; Tan, W.; Shi, F. Catalytic Asymmetric Construction of Axially Chiral Indole-Based Frameworks: An Emerging Area. *Chem. – Eur. J.* **2020**, *26* (68), 15779–15792. (b) He, C.; Hou, M.; Zhu, Z.; Gu, Z. Enantioselective Synthesis of Indole-Based Biaryl Atropoisomers via Palladium-Catalyzed Dynamic Kinetic Intramolecular C-H Cyclization. *ACS Catal.* **2017**, *7* (8), 5316-5320.
(24) Hu, Y.-L.; Wang, Z.; Yang, H.; Chen, J.; Wu, Z.-B.; Lei, Y.; Zhou, L. Conversion of Two Stereocenters to One or Two Chiral Axes: Atroposelective Synthesis of 2,3-Diarylbenzoindoles. *Chem. Sci.* **2019**, *10* (28), 6777–6784.
(25) (a) He, Y.-P.; Wu, H.; Wang, Q.; Zhu, J. Palladium-Catalyzed Enantioselective Cacchi Reaction: Asymmetric Synthesis of Axially Chiral 2,3-Disubstituted Indoles. *Angew. Chem. Int. Ed.* **2020**, *59* (5), 2105–2109. (b) Peng, L.; Li, K.; Xie, C.; Li, S.; Xu, D.; Qin, W.; Yan, H. Organocatalytic Asymmetric Annulation of Ortho-Alkynylanilines: Synthesis of Axially Chiral Naphthyl-C2-Indoles. *Angew. Chem. Int. Ed.* **2019**, *58* (48), 17199–17204.
(26) (a) Gao, K.; Lee, P.-S.; Long, C.; Yoshikai, N. Cobalt-Catalyzed Ortho-Arylation of Aromatic Imines with Aryl Chlorides. *Org. Lett.* **2012**, *14* (16), 4234–4237. (b) Fallon, B. J.; Derat, E.; Amatore, M.; Aubert, C.; Chemla, F.; Ferreira, F.; Perez-Luna, A.; Petit, M. C2-Alkylation and Alkenylation of Indoles Catalyzed by a Low-Valent Cobalt Complex in the Absence of Reductant. *Org. Lett.* **2016**, *18* (9), 2292–2295. (c) Punji, B.; Song, W.; Shevchenko, G. A.; Ackermann, L. Cobalt-Catalyzed C-H Bond Functionalizations with Aryl and Alkyl Chlorides. *Chem. – Eur. J.* **2013**, *19* (32), 10605–10610.
(27) (a) Janssen-Müller, D.; Schlepphorst, C.; Glorius, F. Privileged Chiral N-Heterocyclic Carbene Ligands for Asymmetric Transition-Metal Catalysis. *Chem. Soc. Rev.* **2017**, *46* (16), 4845–4854. (b) Thongpaen, J.; Manguin, R.; Baslé, O. Chiral *N*-Heterocyclic Carbene Ligands Enable Asymmetric C-H Bond Functionalization. *Angew. Chem. Int. Ed.* **2020**, *59* (26), 10242–10251.
(28) Loup, J.; Zell, D.; Oliveira, J. C. A.; Keil, H.; Stalke, D.; Ackermann, L. Asymmetric Iron-Catalyzed C–H Alkylation Enabled by Remote Ligand Meta-Substitution. *Angew. Chem. Int. Ed.* **2017**, *56* (45), 14197–14201.
(29) a) Sherikar, M. S.; Devarajappa, R.; Prabhu, K. R. Weak Coordinating Carbonyl-Directed Rhodium(III)-Catalyzed C-H Activation at the C4-Position of Indole with Allyl Alcohols. *J. Org. Chem.* **2020**, *85* (8), 5516-5524. b) Kalepu, J.; Gandeepan, P.; Ackermann, L.; Pilarski, L. C4-H Indole Functionalisation: Precedent and Prospects. *Chem. Sci.* **2018**, *9* (18), 4203-4216.
(30) (a) Grimme, S.; Ehrlich, S.; Goerigk, L. Effect of the Damping Function in Dispersion Corrected Density Functional Theory. *J. Comput. Chem.* **2011**, *32* (7), 1456–1465. (b) Weigend, F. Accurate Coulomb-Fitting Basis Sets for H to Rn. *Phys. Chem. Chem. Phys.* **2006**, *8* (9), 1057–1065. (c) Zhao, Y.; Truhlar, D. G. Design of Density Functionals That Are Broadly Accurate for Thermochemistry, Thermochemical Kinetics, and Nonbonded Interactions. *J. Phys. Chem. A* **2005**, *109* (25), 5656–5667. (d) Caldeweyher, E.; Ehlert, S.; Hansen, A.; Neugebauer, H.; Spicher, S.; Bannwarth, C.; Grimme, S. A Generally Applicable Atomic-Charge Dependent London Dispersion Correction. *J. Chem. Phys.* **2019**, *150* (15), 154122.
(31) A mechanism through an Co(0) intermediate can not unambiguously be ruled out.
(32) Bursch, M.; Caldeweyher, E.; Hansen, A.; Neugebauer, H.; Ehlert, S.; Grimme, S. Understanding and Quantifying London Dispersion Effects in Organometallic Complexes. *Acc. Chem. Res.* **2019**, *52* (1), 258–266.